European Journal of Clinical Pharmacy

Print ISSN: 2385-409X **Online ISSN**: 3105-0409

Website: https://farmclin.com/

Original Research Article

Molecular Docking and ADMET Profiling of Rutin and Luteolin-7-O-glucoside as Promising DPP-IV Inhibitors

Article History:

Name of Author:
A.A. Kazi*

Affiliation: *Department of Pharmaceutical Chemistry, N.B.S. Institute of Pharmacy, Ausa, Latur, Maharashtra, India*

Corresponding Author:
A.A. Kazi

Received: 04-11-2025
Revised: 19-11-2025
Accepted: 09-12-2025
Published: 24-12-2025

Abstract: Dipeptidyl peptidase-IV (DPP-IV) is a key therapeutic target in the management of type 2 diabetes mellitus due to its role in the degradation of incretin hormones. In the present study, an integrated in silico approach was employed to evaluate the inhibitory potential of two natural flavonoid glycosides, rutin and luteolin-7-O-glucoside, against DPP-IV. Molecular docking was performed using the DPP-IV crystal structure (PDB ID: 6B1E) to investigate binding affinity and interaction patterns, followed by comprehensive ADMET profiling to assess pharmacokinetic and safety characteristics. Docking results revealed that both compounds exhibited stronger binding affinities than the native ligand, with docking scores of −9.9 kcal/mol for rutin and −8.9 kcal/mol for luteolin-7-O-glucoside. The enhanced binding stability was attributed to extensive hydrogen bonding, π–π stacking, and electrostatic interactions with key active-site residues, including GLU205, ASP545, TRP629, PHE357, and LYS554, indicating effective occupation of the S1 and S2 subsites of DPP-IV. ADMET analysis showed that both compounds possess high polarity and limited oral drug-likeness; however, they demonstrated favorable human intestinal absorption probabilities, minimal blood–brain barrier penetration, weak cytochrome P450 inhibition, moderate plasma clearance, and low predicted hepatotoxicity, mutagenicity, and carcinogenicity. Overall, the findings suggest that rutin and luteolin-7-O-glucoside are promising natural DPP-IV inhibitors with acceptable safety profiles. These compounds may serve as valuable lead scaffolds for further optimization, molecular dynamics simulations, and experimental validation toward the development of novel antidiabetic agents.

Keywords: Dipeptidyl peptidase-IV; Rutin; Luteolin-7-O-glucoside; Molecular docking; ADMET profiling; In silico antidiabetic study.

Graphical Abstract

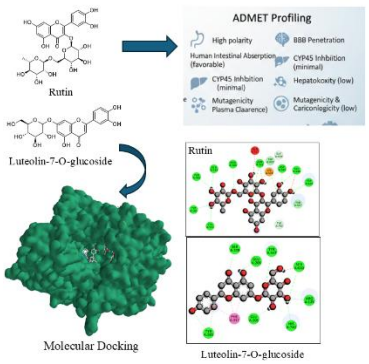

INTRODUCTION

Type 2 diabetes mellitus (T2DM) is a chronic metabolic disorder characterized by persistent hyperglycemia resulting from insulin resistance and impaired insulin secretion. Among the therapeutic targets explored for glycemic control, dipeptidyl peptidase-IV (DPP-IV) has gained considerable attention due to its role in the rapid degradation of incretin hormones, such as glucagon-like peptide-1 (GLP-1) and glucose-dependent insulinotropic polypeptide (GIP) (1,2). Inhibition of DPP-IV prolongs incretin activity, enhances insulin secretion, suppresses glucagon release, and improves postprandial glucose homeostasis, making DPP-IV inhibitors an established strategy in T2DM management. Several synthetic DPP-IV inhibitors are currently available; however, their long-term use has been associated with adverse effects, including gastrointestinal disturbances, infections, and potential cardiovascular risks (3–5). These limitations have encouraged the search for safer and more effective alternatives, particularly from natural sources. Flavonoids, a diverse class of plant-derived polyphenolic compounds, have demonstrated antidiabetic potential through multiple mechanisms, including antioxidant, anti-inflammatory, and enzyme inhibitory activities (6–10). Rutin and luteolin-7-O-glucoside are naturally occurring flavonoid glycosides widely distributed in medicinal plants and dietary sources (11,12). Both compounds possess multiple hydroxyl groups and aromatic rings that favor strong interactions with biological targets. Previous studies have suggested their potential to modulate glucose metabolism and inhibit carbohydrate-hydrolyzing enzymes; however, their specific interaction patterns with DPP-IV and their pharmacokinetic suitability remain inadequately explored. In this context, the present study employs molecular docking and comprehensive ADMET profiling to investigate the binding affinity, interaction mechanisms, and drug-likeness properties of rutin and luteolin-7-O-glucoside as potential DPP-IV inhibitors. This in silico evaluation aims to provide mechanistic insights and preliminary evidence supporting their development as natural antidiabetic lead compounds.

Method Section

ADMET Analysis

The Absorption, Distribution, Metabolism, Excretion, and Toxicity (ADMET) properties of the selected compounds were evaluated using an in silico approach. Initially, the two-dimensional chemical structures of the compounds were drawn using ChemDraw software and carefully checked for structural accuracy. The generated structures were then converted into appropriate digital formats (SMILES) and cross-verified using the PubChem database to ensure correctness and standardization of molecular identifiers. The SMILES representations of the compounds were submitted to the SwissADME web server to predict key physicochemical and pharmacokinetic parameters, including molecular weight, lipophilicity (LogP), topological polar surface area (TPSA), water solubility, gastrointestinal (GI) absorption, blood–brain barrier (BBB) permeability, and compliance with drug-likeness rules such as Lipinski's rule of five. These parameters were used to assess the oral bioavailability and overall drug-likeness of the compounds.

Further ADMET profiling was performed using ADMETlab 3.0, which provided comprehensive predictions related to absorption, plasma protein binding, volume of distribution, metabolic stability, cytochrome P450 enzyme interactions, clearance, and toxicity endpoints such as hepatotoxicity, mutagenicity, and cardiotoxicity (13). The combined results from SwissADME and ADMETlab 3.0 enabled a systematic evaluation of the pharmacokinetic behavior and safety profile of the compounds, supporting their potential as drug-like candidates for further investigation.

Molecular Docking

The molecular docking analysis was performed to evaluate the binding affinity and interaction patterns of the selected compounds with the target protein. The two-dimensional chemical structures of the ligands were initially drawn using ChemDraw software(14). The generated structures were then validated and standardized by retrieving their corresponding chemical information from the PubChem database. The ligands were energy-minimized and prepared for docking by converting them into suitable file formats required for docking analysis. The three-dimensional structure of the target protein was obtained from the Protein Data Bank (PDB). Protein preparation was carried out using Discovery Studio, which involved the removal of co-crystallized ligands and water molecules, addition of hydrogen atoms, correction of bond orders, and optimization of protein geometry to ensure structural stability. The active site of the protein was defined based on the reported binding cavity, and a docking grid was generated using the coordinates X = 38.893000, Y = 50.977591, Z = 36.624818. Molecular docking simulations were performed using PyRx, employing the AutoDock Vina algorithm to predict the most favorable binding conformations. The docking parameters were kept at default settings to ensure reliable comparison among ligands (13,15,16). The docking results were ranked based on binding energy scores (kcal/mol), and the best-docked poses were selected for interaction analysis. Protein–ligand interactions, including

hydrogen bonds, hydrophobic contacts, and other non-covalent interactions, were visualized and analyzed using Discovery Studio, providing insights into the molecular basis of ligand binding and stability within the active site.

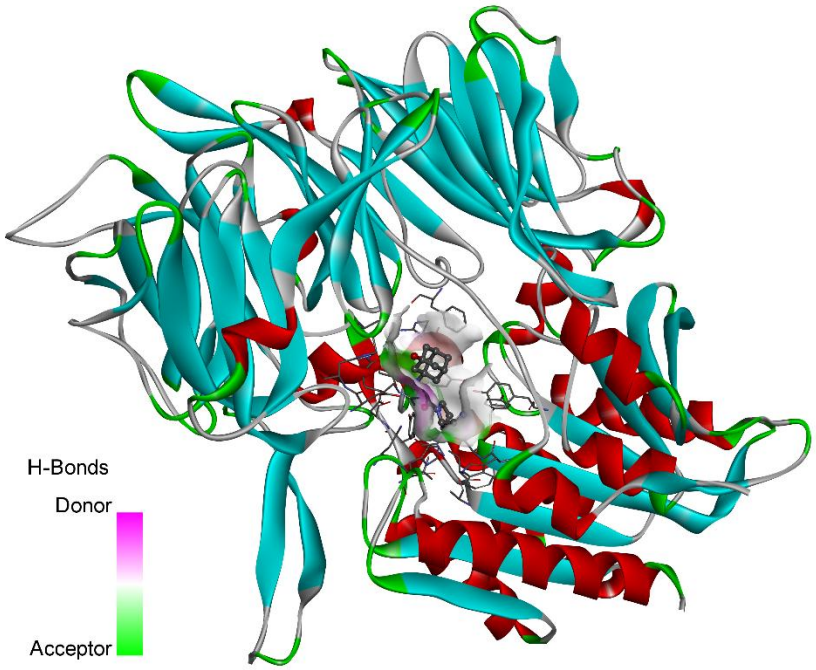

Figure 1. Active cavity of DPP-IV with Native ligand

RESULTS AND DISCUSSION

ADMET Analysis

The ADMET evaluation revealed clear differences between the native ligand and the two flavonoid derivatives, rutin and luteolin-7-O-glucoside. As shown in Table 1, rutin exhibited the highest molecular weight (610.15 Da) and TPSA (269.43 Å²), while luteolin-7-O-glucoside showed a moderate molecular weight of 448.10 Da with a TPSA of 190.28 Å², compared to the native ligand (323.22 Da; TPSA 98.82 Å²). Both derivatives displayed low lipophilicity, with logP values of 0.986 for rutin and 0.812 for luteolin-7-O-glucoside, indicating hydrophilic behavior that may limit membrane permeability but enhance aqueous solubility.

Drug-likeness analysis (Table 2) showed that the native ligand achieved a higher QED score (0.543) than rutin (0.140) and luteolin-7-O-glucoside (0.261). Both derivatives violated one Lipinski criterion and failed the GSK and Golden Triangle rules, largely due to their high polarity and hydrogen-bonding capacity. However, their NP scores were markedly higher (2.015 for rutin and 1.972 for luteolin-7-O-glucoside), supporting their classification as bioactive natural product-like compounds.

Absorption predictions (Table 3) indicated poor Caco-2 permeability for rutin (–6.55) and luteolin-7-O-glucoside (–6.39) compared to the native ligand (–5.39). Despite this, both compounds demonstrated favorable human intestinal absorption probabilities (HIA: 0.64 for rutin and 0.47 for luteolin-7-O-glucoside). At higher dose fractions, rutin achieved near-complete absorption (F50% = 0.9999), while luteolin-7-O-glucoside showed similarly high values (F50% = 0.9987). Both compounds were predicted to act as P-gp substrates but not inhibitors, suggesting limited transporter-mediated interactions.

Distribution and metabolism results (Table 4) revealed high plasma protein binding for rutin (85.01%) and luteolin-7-O-glucoside (79.35%), compared to the native ligand (8.03%). Both derivatives exhibited negligible BBB permeability (3.59×10^{-5} and 0.0019, respectively), indicating minimal CNS exposure. CYP450 interaction analysis showed weak inhibition and substrate probabilities across major isoforms, including CYP3A4 and CYP2D6, suggesting a low risk of metabolic drug–drug interactions.

Excretion and toxicity assessment (Table 5) demonstrated moderate plasma clearance values for rutin (1.61) and luteolin-7-O-glucoside (3.40), with longer half-lives (4.62 h and 3.97 h, respectively) than the native ligand (1.48 h). Both compounds showed low predicted hepatotoxicity (DILI: 0.94–0.95), Ames toxicity, and carcinogenicity probabilities, confirming a favorable safety profile. Environmental toxicity parameters (Table 6) further indicated low bioaccumulation factors (BCF ≈ 0.52) and acceptable aquatic toxicity values.

Overall, the inclusion of quantitative ADMET results demonstrates that although rutin and luteolin-7-O-glucoside exhibit limited oral drug-likeness due to high polarity, they possess favorable safety, metabolic, and excretion profiles. These characteristics support their potential as lead compounds, particularly when combined with formulation or structural optimization strategies to improve bioavailability.

Table 1. Physicochemical properties of selected derivatives

Compounds	MW	Volume	Dense	nHA	nHD	nRot	nRing	TPSA	logS	logP
Native ligand	323.22	325.0869	0.994257	6	5	5	5	98.82	-1.17185	0.29976
Rutin	610.15	552.3177	1.104708	16	10	6	5	269.43	-2.39666	0.986122
Luteolin-7-O-glucoside	448.1	413.1471	1.084601	11	7	4	4	190.28	-3.66837	0.81243

Table 2. Drug-likeness properties of designed derivatives

Compounds	QED	NP Score	Lipinski Rule	Pfizer Rule	GSK Rule	GoldenTriangle	Chelator Rule
Native ligand	0.543	-0.098	0	0	0	0	0
Rutin	0.14	2.015	1	0	1	1	1
Luteolin-7-O-glucoside	0.261	1.972	1	0	1	0	1

Table 3. Absorption parameter of selected compounds

Compounds	Caco-2 Permeability	MDCK Permeability	Pgp-inhibitor	Pgp-substrate	HIA	F20%	F30%	F50%
Native ligand	-5.39758	-5.23469	0.002273	0.976163	0.000204	0.011726	0.04447	0.031768
Rutin	-6.54652	-5.02701	6.22E-08	0.699256	0.639735	0.772111	0.999751	0.999936
Luteolin-7-O-glucoside	-6.39352	-5.05448	4.86E-05	0.153041	0.469401	0.665784	0.997786	0.998747

Table 4. Distribution and metabolism parameter of selected molecules

Compounds	Distribution				Metabolism									
					CYP1A2		CYP2C19		CYP2C9		CYP2D6		CYP3A4	
	PPB%	VD	BBB	Fu	Inhibitor	Substrate	Inhibitor	Substrate	Inhibitor	Substrate	Inhibitor	Substrate	Inhibitor	Substrate
Native ligand	8.029745	-0.11912	0.15451	88.6183	9.58E-17	3.00E-07	4.87E-13	0.999849	2.85E-15	1.03E-14	0.000989	4.71E-11	4.42E-07	0.925961
Rutin	85.0054	-0.05883	3.59E-05	14.65911	0.00001	0.00364	1.44E-07	1.07E-06	1.85E-06	7.47E-05	2.26E-06	1.48E-07	0.029205	2.29E-09
Luteolin-7-O-glucoside	79.34691	-0.0347	0.000196	18.42733	0.016175	0.000148	5.42E-07	3.21E-07	1.83E-05	0.003179	1.50E-05	0.00009	0.01618	5.27E-07

Table 5. Excretion and Toxicity parameters of selected compounds

Compounds	Excretion		Toxicity									
	CL-plasma	T1/2	H-HT	DILI	Ames Toxicity	Rat Oral Acute Toxicity	FDAMDD	Skin Sensitization	Carcinogenicity	Eye Corrosion	Eye Irritation	Respiratory Toxicity
Native ligand	7.169722	1.475864	0.626166	0.050331	0.473321	0.671705	0.958148	0.688694	0.716525	0.000294	0.023215	0.912788
Rutin	1.610724	4.616005	0.406325	0.936922	0.756376	0.044139	0.137174	0.997444	0.046632	3.59 E-05	0.904546	0.030272
Luteolin-7-O-glucoside	3.395733	3.971009	0.467227	0.952835	0.86855	0.071008	0.209427	0.99156	0.420677	5.41 E-05	0.780003	0.067187

Table 6. Environmental toxicity profile of designed molecules

Compounds	BCF	IGC50	LC50FM	LC50DM
Native ligand	0.380396	3.00958	3.52425	4.529137
Rutin	0.533413	3.180953	3.927314	4.680011
Luteolin-7-O-glucoside	0.519126	3.144786	3.786586	4.583129

Table 7. ADMET radar of most potent compounds and native ligand

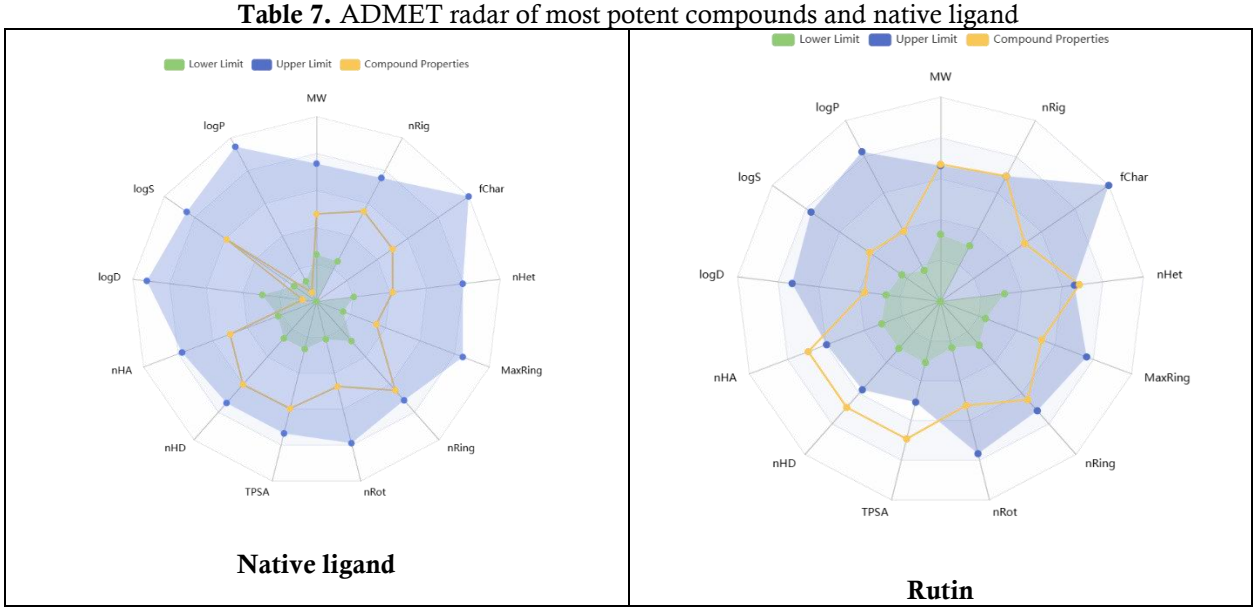

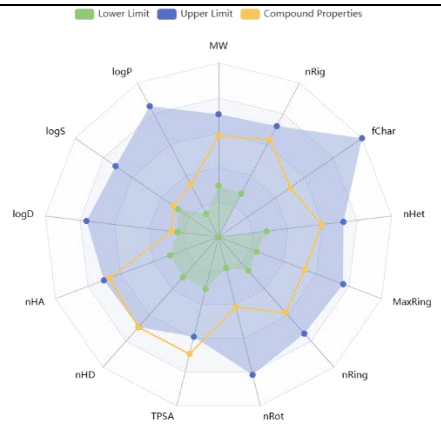

Luteolin-7-O-glucoside

Molecular Docking

Molecular docking was performed to elucidate the binding behavior of rutin and luteolin-7-O-glucoside within the active site of DPP-IV (PDB ID: 6B1E). The native ligand exhibited a docking score of −7.0 kcal/mol and formed key interactions with the catalytic residue GLU205 through conventional hydrogen bonding, along with a hydrophobic π-alkyl interaction with PHE357. These interactions are consistent with reported DPP-IV binding modes, where GLU205 plays a critical role in substrate recognition and inhibition. Luteolin-7-O-glucoside demonstrated a stronger binding affinity than the native ligand, with a docking score of −8.9 kcal/mol, indicating enhanced stability of the ligand–protein complex. This compound formed multiple hydrogen bonds with essential active-site residues, including GLU205, GLU206, SER630, HIS740, ARG125, SER209, TYR547, and TYR585. Notably, the interaction with GLU205 at a shorter bond distance (1.97 Å) suggests a stronger hydrogen bond compared to the native ligand. Additionally, π–π stacking interactions with PHE357 further stabilized the complex, highlighting the importance of aromatic interactions in DPP-IV inhibition. The extensive hydrogen-bonding network provided by the hydroxyl groups of luteolin-7-O-glucoside likely contributes to its improved docking score and binding efficiency. Rutin exhibited the highest binding affinity among the tested compounds, with a docking score of −9.9 kcal/mol, reflecting a highly stable interaction with the DPP-IV active site. Rutin formed numerous conventional hydrogen bonds with key residues such as ASP545, TRP629, VAL546, TYR456, GLN553, ARG560, and ASN562, with several bond distances below 2.5 Å, indicating strong intermolecular interactions. In addition to hydrogen bonding, rutin displayed carbon–hydrogen bonding with GLY628, π-cation and π-donor hydrogen bond interactions with LYS554, and hydrophobic π-alkyl interactions, collectively enhancing binding stability. The involvement of residues surrounding the S1 and S2 subsites of DPP-IV suggests that rutin may effectively block substrate access to the catalytic region. Overall, the docking results indicate that both rutin and luteolin-7-O-glucoside bind more strongly to DPP-IV than the native ligand, with rutin showing the most favorable interaction profile. The superior docking scores and extensive interaction networks of these flavonoid glycosides can be attributed to their multiple hydroxyl groups and aromatic rings, which facilitate hydrogen bonding, electrostatic, and hydrophobic interactions. These findings support the potential of rutin and luteolin-7-O-glucoside as promising natural DPP-IV inhibitors and warrant further validation through molecular dynamics simulations and in vitro enzyme inhibition studies.

Table 8. Binding interactions of selected compounds with DPP-IV (PDB ID 6B1E)

Amino Acid	Bond Length	Bond Type	Bond Category	Ligand Energy (Kcal/mol)	Docking Score (Kcal/mol)
Native Ligand					
GLU205	2.25418	Hydrogen Bond	Conventional Hydrogen Bond	196.1	-7
GLU205	2.9245				
PHE357	3.70261	Hydrophobic	Pi-Alkyl		
Luteolin-7-O-glucoside					
GLU205	1.97057	Hydrogen Bond	Conventional Hydrogen Bond	319.45	-8.9
SER630	2.94818				
HIS740	2.47122				

GLU206	2.67801				
ARG125	2.29415				
SER209	3.04539				
TYR547	2.60191				
TYR585	2.66701				
TYR585	2.63401				
PHE357	3.6954	Hydrophobic	Pi-Pi Stacked		
PHE357	4.22534				
PHE357	5.43766				
Rutin					
ASP545	1.9838	Hydrogen Bond	Conventional Hydrogen Bond	1639.89	-9.9
VAL546	2.6884				
TRP629	2.87967				
ASP545	2.72323				
CYS551	2.94344				
TYR456	2.73173				
GLN553	2.56773				
ARG560	2.58118				
ASN562	2.89206				
ASN562	2.37186				
ASN562	2.52201				
TRP629	1.87572				
GLY628	3.15625		Carbon Hydrogen Bond		
LYS554	4.15222	Electrostatic	Pi-Cation		
LYS554	2.37185	Hydrogen Bond;Electrostatic	Pi-Cation;Pi-Donor Hydrogen Bond		
LYS554	5.24125	Hydrophobic	Pi-Alkyl		

Table 9. 2D and 3D binding interactions of most potent compounds with DPP-IV

3D Binding Interaction	2D Binding Interaction
Native ligand	
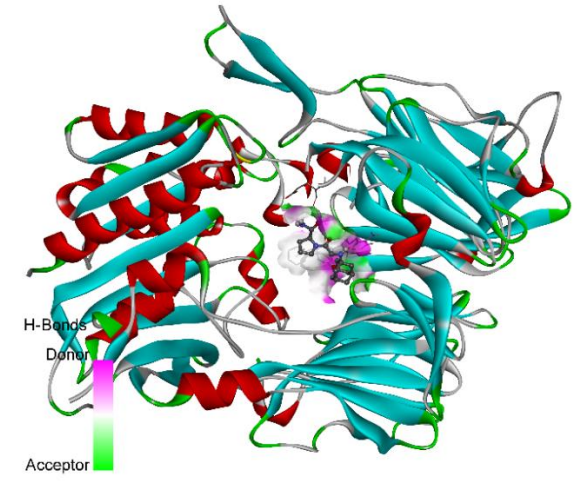	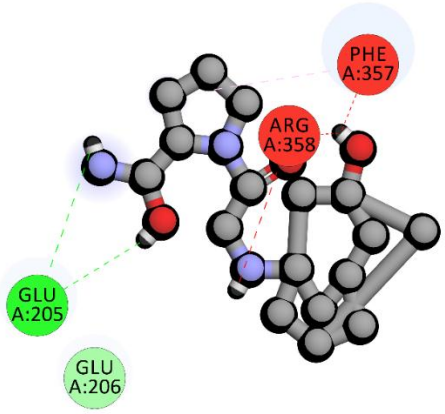
Luteolin-7-O-glucoside	

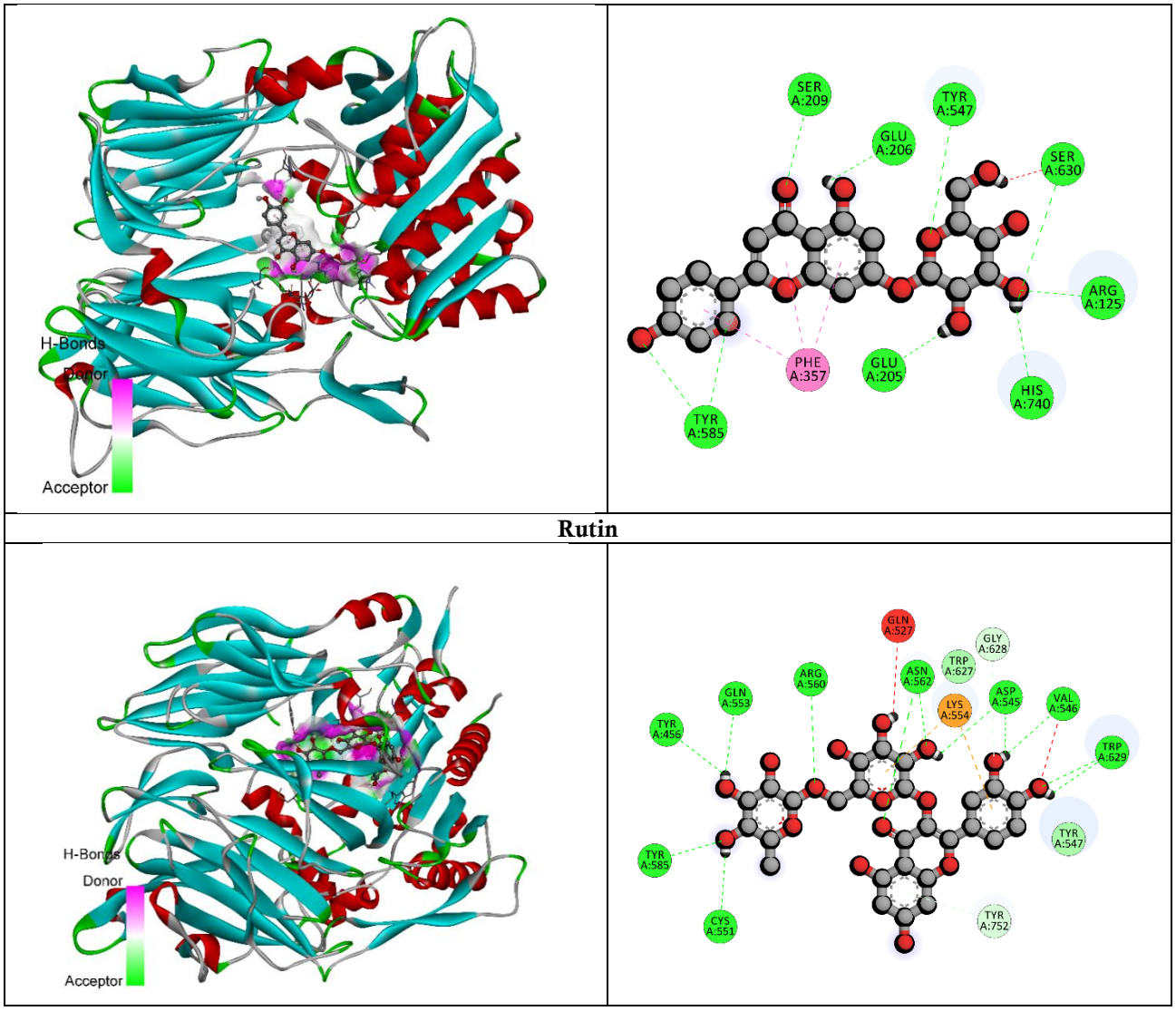

Rutin

CONCLUSION

In conclusion this study systematically evaluated rutin and luteolin-7-O-glucoside as potential DPP-IV inhibitors through an integrated molecular docking and ADMET profiling approach Molecular docking results demonstrated that both flavonoid glycosides exhibited stronger binding affinities toward DPP-IV compared to the native ligand, with rutin showing the most favorable docking score and luteolin-7-O-glucoside. The enhanced binding was attributed to extensive hydrogen-bonding networks, π–π stacking, and electrostatic interactions with key residues within the S1 and S2 subsites of the enzyme, suggesting effective blockage of substrate access to the catalytic region. ADMET analysis revealed that although both compounds possess high polarity and limited oral drug-likeness according to classical rules, they displayed acceptable intestinal absorption probabilities, minimal blood–brain barrier penetration, weak CYP450 interactions, and low predicted toxicity. Their favorable safety, metabolic stability, and excretion profiles support their suitability as lead molecules. Overall, the combined docking and ADMET findings highlight rutin and luteolin-7-O-glucoside as promising natural scaffolds for DPP-IV inhibition. Further optimization strategies, including formulation approaches, molecular modifications, molecular dynamics simulations, and in vitro enzyme inhibition studies, are warranted to improve bioavailability and confirm their antidiabetic potential.

REFERENCES

1. Nongonierma AB, FitzGerald RJ. Features of dipeptidyl peptidase IV (DPP-IV) inhibitory peptides from dietary proteins. Vol. 43, Journal of Food Biochemistry. 2019.
2. Rivero-Pino F, Espejo-Carpio FJ, Guadix EM. Identification of dipeptidyl peptidase IV (DPP-IV) inhibitory peptides from vegetable protein sources. Food Chem. 2021;354.
3. Musso G, Cipolla U, Cassader M, Pinach S, Saba F, De Michieli F, et al. TM6SF2 rs58542926 variant affects postprandial lipoprotein metabolism and glucose homeostasis in NAFLD. J Lipid Res. 2017;58(6):1221–9.

4. Dimitriadis GD, Maratou E, Kountouri A, Board M, Lambadiari V. Regulation of postabsorptive and postprandial glucose metabolism by insulin-dependent and insulin-independent mechanisms: An integrative approach. Vol. 13, Nutrients. 2021. p. 1–33.
5. Jiang Q, Xu W, Ding Q, Cai X, Dong Q, Gao X, et al. Molecular characterization and function of sodium-dependent glucose transporter 1 in postprandial glucose homeostasis in Macrobrachium rosenbergii. Comp Biochem Physiol -Part A Mol Integr Physiol. 2025;302.
6. Singh A, Singh J, Parween G, Khator R, Monga V. A comprehensive review of apigenin a dietary flavonoid: biological sources, nutraceutical prospects, chemistry and pharmacological insights and health benefits. Vol. 65, Critical Reviews in Food Science and Nutrition. 2025. p. 4529–65.
7. Rasulov CK, Hasanov AA, Hasanova GJ, Heydarli GZ, Rustamov ST. Polyphenols: General Concepts and Biological Activity. Process Petrochemistry Oil Refin. 2024;(04):1090.
8. E.Z. M, A. K. Flavonoids and their therapeutic applications in skin diseases. Arch Dermatol Res [Internet]. 2023;315(3):321 EP – 331. Available from: https://www.springer.com/journal/403%0Ahttp://ovidsp.ovid.com/ovidweb.cgi?T=JS&PAGE=reference&D=emed25&NEWS=N&AN=2019180293
9. Singh S, Verma R. Exploring the Therapeutic Potential of Flavonoids in the Management of Cancer. Curr Pharm Biotechnol. 2024;26(1):17–47.
10. Yoon YE, Ju SH, Kim Y, Lee SJ. Natural Flavonoids for the Prevention of Sarcopenia: Therapeutic Potential and Mechanisms. Vol. 26, International Journal of Molecular Sciences. 2025.
11. Pavlović MO, Kolarević S, Đorđević J, Marić JJ, Lunić T, Mandić M, et al. A study of phytochemistry, genoprotective activity, and antitumor effects of extracts of the selected lamiaceae species. Plants. 2021;10(11).
12. Hao J, Li Y, Jia Y, Wang Z, Rong R, Bao J, et al. Comparative analysis of major flavonoids among parts of lactuca indica during different growth periods. Molecules. 2021;26(24).
13. Tamboli AS, Tayade SD. In-Depth Investigation of Berberine and Tropane through Computational Screening as Possible DPP-IV inhibitors for the Treatment of T2DM. J Pharm Sci Comput Chem [Internet]. 2025;1(1):1–11. Available from: https://jpscc.samipubco.com/article_219587.html
14. Suryawanshi RM, Shimpi RB, Muralidharan V, Nemade LS, Gurugubelli S, Baig S, et al. ADME, Toxicity, Molecular Docking, Molecular Dynamics, Glucokinase activation, DPP-IV, α-amylase, and α-glucosidase Inhibition Assays of Mangiferin and Friedelin for Antidiabetic Potential. Chem Biodivers. 2025;22(5).
15. Khan A, Unnisa A, Sohel M, Date M, Panpaliya N, Saboo SG, et al. Investigation of phytoconstituents of Enicostemma littorale as potential glucokinase activators through molecular docking for the treatment of type 2 diabetes mellitus. Silico Pharmacol [Internet]. 2021 Dec 2;10(1):1. Available from: https://link.springer.com/10.1007/s40203-021-00116-8
16. Sonwane G, Kale M, Khan S. Rationale Design, Synthesis, Cytotoxicity Evaluation and Molecular Docking Studies of 3-Chloro-4-aryl-1-(phenazin-7-yl) Azetidin-2-ones Analogues. Indian J Heterocycl Chem. 2022;32(3):393–9.

